ADVANCED FUNCTIONAL MATERIALS
www.afm-journal.de

Materials Views
www.MaterialsViews.com

# Dramatic Structural Enhancement of Chirality in Photopatternable Nanocomposites of Chiral Poly(fluorene-*alt*-benzothiadiazole) (PFBT) in Achiral SU-8 Photoresist

*Heong Sub Oh, Hongsub Jee, Alexander Baev, Mark T. Swihart,* and Paras N. Prasad**

**Materials with large optical activity at visible wavelengths are of great interest in photonics, particularly as one of the routes towards optical metamaterials. Here, dramatic structural enhancement of the optical activity of chiral poly(fluorene-*alt*-benzothiadiazole) (PFBT) when dispersed in SU-8 to form a nanocomposite is reported. The supramolecular helical organization of PFBT chains in these optically clear nanocomposite films produces specific rotation at visible wavelengths that is 68 times that of a pure chiral PFBT film of the same optical absorbance. Photopatterning and development under standard conditions for SU-8 leave behind a residual film of dispersed PFBT/SU-8 aggregates in the nominally unexposed regions where the SU-8 matrix is removed. After annealing, the patterned film exhibits specific rotation 58 times that of a pure chiral PFBT film of the same optical absorbance. Photopatterned and annealed films have a dissymmetry ratio as high as $|g_{abs}| = 0.32$. This dramatic enhancement is attributed to supramolecular helical organization of the aggregates within the nanocomposites and of the aggregates liberated from the SU-8 matrix in the exposed regions.**

## 1. Introduction

Optically active polymeric materials are of interest in a variety of contexts,[1–9] but are particularly promising as a route to producing optical metamaterials. In a chiral medium, the effective refractive index for circularly polarized light is given by

$$n_{\text{eff}} = \sqrt{\varepsilon\mu} \pm \kappa \quad (1)$$

where $\mu$ and $\varepsilon$ are the magnetic permeability and electrical permittivity, respectively, and $\kappa$ is the chirality parameter.[6] This implies that for one circular polarization, the effective refractive index could be made negative, zero, or near-zero without achieving negative values of $\mu$ and $\varepsilon$.[10–12] Unfortunately, values of $\kappa$ in naturally occurring homogeneous media are far too small to have a practical effect (typically below 0.001)[11,13] and most often peak at ultraviolet wavelengths. Chiral conjugated polymers, especially co-polymers with a donor-acceptor structure similar to the chiral PFBT studied here, can have optical transitions in the visible spectrum, and concomitantly can exhibit maximum values of $\kappa$ at visible wavelengths.[14,15] Plasmonic enhancement of chirality in such films can be achieved by doping them with gold nanoparticles, as we have recently demonstrated.[15] Purely structural enhancement of chirality, by helical supramolecular organization of the polymer chains, is also possible, and that effect is exploited in the present work. Although the enhancement of chirality of $\pi$-conjugated polymers by enantioselective interactions with small chiral molecules is known, the relationship between the optical properties and supramolecular ordering of copolymers in the solid state remains relatively unexplored.

Structural and optical characterization of self-assembling chiral molecules in solution has been reported.[16] Induced chirality in optically active molecules could be sensitively controlled by solvent, temperature, pH and the presence of solvent vapor.[17,18] When such molecules are dissolved in nonpolar solvents, their chirality is altered upon addition of a protic solvent such as methanol or a polar solvent such as DMF into a good solvent. This is attributed to aggregation and helical

Dr. H. S. Oh, H. Jee, Prof. A. Baev,
Prof. M. T. Swihart, Prof. P. N. Prasad
Institute for Lasers
Photonics and Biophotonics
University at Buffalo
The State University of New York
Buffalo, NY 14260, USA
E-mail: swihart@buffalo.edu; pnprasad@buffalo.edu
H. Jee, Prof. P. N. Prasad
Department of Electrical Engineering
University at Buffalo
The State University of New York
Buffalo, NY 14260, USA
Prof. M. T. Swihart
Department of Chemical and Biological Engineering
University at Buffalo
The State University of New York
Buffalo, NY 14260, USA
Prof. P. N. Prasad
Department of Chemistry
University at Buffalo
The State University of New York
Buffalo, NY 14260, USA

DOI: 10.1002/adfm.201201273


© 2012 WILEY-VCH Verlag GmbH & Co. KGaA, Weinheim

self-assembly as the solvent quality worsens. In solids, changes in the chiroptical properties of molecules can be induced by annealing.[5,6] As we previously reported, optical activity of pure chiral PFBT films and that of chiral PFBT/gold nanoparticle composites was greatly enhanced upon annealing.[15] In that case, the absolute optical activity in annealed nanocomposites, characterized by the chirality parameter, $\kappa$, was more than three orders of magnitude higher than that of pure PFBT prior to annealing. This overall effect resulted from both structural and plasmonic enhancement of chirality.

To the best of our knowledge, amplification of chirality in the solid phase by dispersion of a chiral polymer in a photopolymerizable matrix has not been previously reported. Herein, we report the extraordinary optical activity achieved in thin films upon doping of SU-8 photoresist with a chiral $\pi$-conjugated copolymer, PFBT. Optical activity of the chiral polymer in the PFBT/SU-8 nanocomposite thin film is dramatically higher than that of an equivalent pure PFBT film of the same absorbance. Moreover, the optical activity of chiral polymer aggregates left behind upon removal of the SU-8 matrix is also dramatically higher than that of the equivalent pure PFBT film.

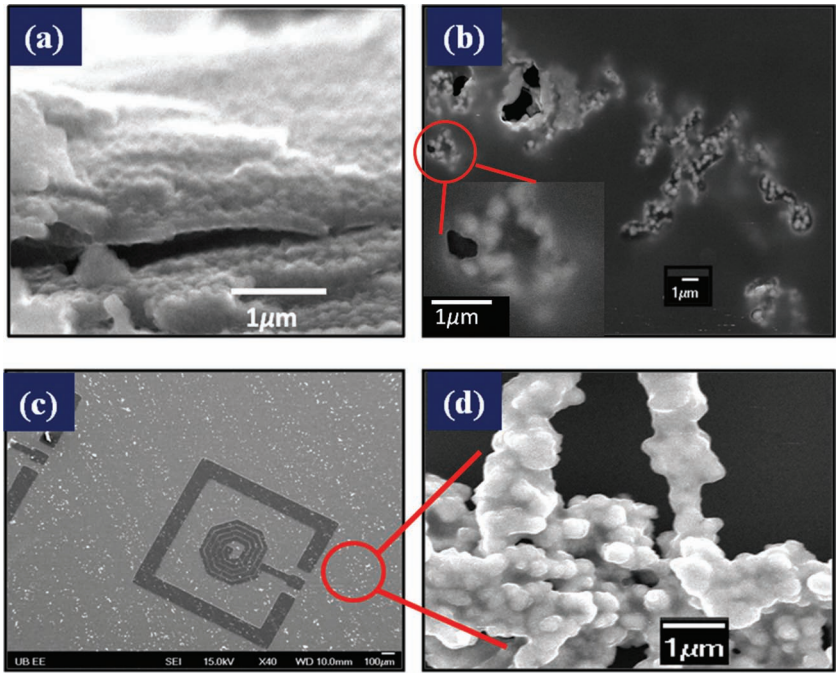


**Figure 1.** SEM images of a) pure PFBT film edge, showing helical fibrils and b) PFBT/SU-8, 1/40 ratio photopolymer film annealed at 150 °C for 15 min, showing helical fibrils embedded in SU-8 matrix. The inset shows an expanded image of the indicated region. c) PFBT/SU-8, 1/40 ratio film after photopatterning, development with PGMEA and annealing at 150 °C for 15 min (lighter gray areas are those in which SU-8 has been removed). d) Expanded image of a nominally unexposed area of the pattern shown in (c).

## 2. Results and Discussion

### 2.1. Dramatic Enhancement of Circular Dichroism in Chiral PFBT/Achiral SU-8 Nanocomposites

Photocured nanocomposites of chiral PFBT/SU-8 were formed by photopolymerization of PFBT in SU-8 at various ratios. Photopolymerization is an established method for fabricating 2D microstructures.[19] The commercially available epoxy-based photoresist SU-8 is optimized for high-aspect-ratio structure fabrication and is well-suited for 3D lithography.[20,21] SU-8 and chiral PFBT were dissolved in mixtures of cyclopentanone (CPO) and tetrahydrofuran (THF) (1:3, *v/v*) then spin coated to form 1.0 to 9.0 μm thick films. After UV exposure, samples were developed with PGMEA (propylene glycol methyl ether acetate) and rinsed with 2-propanol. Films were annealed under inert atmosphere for 15 minutes at various temperatures to promote helical self-assembly of the chiral polymer. The optical density and chirality of the composites were measured using UV-vis absorption and circular dichroism (CD) spectrometry at each stage of the process.

**Figure 1** presents SEM images showing the microstructure of a pure PFBT film (Figure 1a) and photopolymerized nanocomposite films. Figure 1b shows a PFBT aggregate embedded within the SU-8 matrix. Such helical aggregates may form by microscale phase separation, induced either by solvent evaporation or by thermal- or photo-initiated cross-linking of SU-8. Surprisingly, such a nanocomposite film with approximately the same optical density as the pure PFBT film, showed a CD response nearly 44 times larger than that of the pure PFBT film (**Figure 2**a, curves 1 and 2). Note that the PFBT/SU-8 film must be much thicker than the pure PFBT film to achieve the same total absorbance at visible wavelengths. However, because the optical densities are similar, direct comparison of CD response of these films of different thicknesses is justified. The absorption spectrum was almost unchanged upon annealing of the blanket photopolymerized film (Figure 2b, curve 3). Nonetheless, the CD spectrum did change, with the peak CD intensity increasing by about 55%. This change may be attributable to local changes in the PFBT configuration and aggregation state that are not prevented by the rigid photo-crosslinked SU-8 matrix. In contrast, a photopatterned and developed film (Figure 2a, curves 4 and 5) showed a much larger relative increase in CD upon annealing, along with a slight change in absorbance. Before annealing, the CD peak was red-shifted relative to pure PFBT and only 14 times larger than that of pure PFBT. However, after annealing, the film showed an additional 4-fold increase in maximum CD value. The resulting maximum CD value was 58 times that of the pure PFBT film (Figure 2, curve 5), although it was still slightly lower than that of the film annealed without photopolymerization. This can also be expressed as a dissymmetry ratio of $g_{abs} = -0.17$ for the photopatterned and annealed film, slightly smaller than the value of $g_{abs} = -0.26$ for the unpatterned film that was


© 2012 WILEY-VCH Verlag GmbH & Co. KGaA, Weinheim

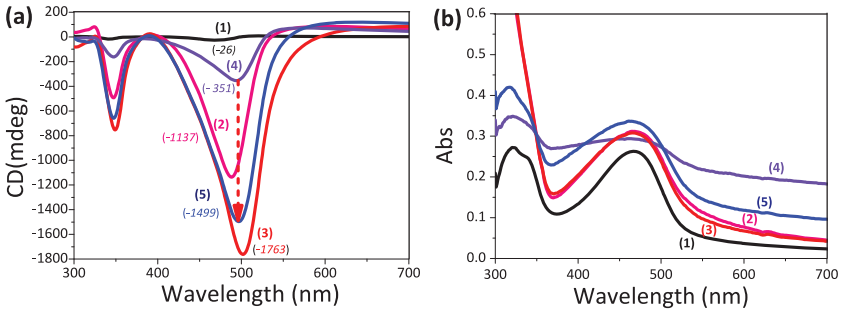


**Figure 2.** a) CD and b) UV-vis absorption spectra of: 1) annealed pure PFBT film and 2–5) PFBT/SU-8, 1/30 mass ratio film spin-coated from 20% solid content solution: 2) after prebaking and blanket photo-polymerization; 3) after prebaking and annealing (thermal-polymerization); 4) after prebaking, patterned photo-polymerization, and developing with PGMEA; and 5) after prebaking, patterned photo-polymerization, developing, and annealing. Prebaking = 95 °C (5 min), annealing temperature ($T_{ann}$) = 150 °C (15 min).

annealed without photopolymerization. Both of these are dramatically higher than the value of $g_{abs} = -0.003$ obtained for the pure PFBT film. Both before and after annealing, the absorption spectrum of the patterned film shows a baseline offset attributed to scattering by the microscale patterned features and by roughness and residual PFBT/SU8 in the UV-unexposed areas. This scattering was reduced after annealing.

Scanning electron microscope (SEM) imaging of photopatterned and developed films (Figure 1c) showed chiral PFBT residue in nominally unexposed areas, i.e., those areas not directly exposed to UV light, in which the SU-8 was therefore not crosslinked and should have been removed during development. The PFBT/SU-8 aggregates in the nominally unexposed regions, where the SU-8 has been removed, exhibited somewhat helical conformations (Figure 1d). This residual film was typically ¼ the thickness of the film in the photo-crosslinked regions. We attribute the large increase in CD after annealing of these developed films to helical self-assembly of these aggregates. Under typical conditions used for photopatterning SU-8, most of the nominally unexposed SU-8 could be removed by washing with PGMEA. However, PFBT, most likely photografted with SU-8, in these areas was not removed. The retention of the PFBT is demonstrated by the negligible decrease in optical density in the visible part of the spectrum, even when 90% of the film area is nominally unexposed (i.e., should nominally have had the film removed). In contrast, PGMEA development of PFBT/SU-8 films that had not been patterned (i.e., that were completely un-exposed) led to near-complete removal of both polymers. This suggests that PFBT, a very strong absorber, served to increase the photosensitivity of the nanocomposite film. Some light may leak under the shadow mask via multiple reflections from the glass substrate. The exposure dose reaching these areas appears to be sufficient to initiate some photografting of SU-8 and PFBT and/or PFBT-initiated SU-8 crosslinking and produce these chiral aggregates that are not removed by standard SU-8 developer. These aggregates, which are not encapsulated in a matrix of crosslinked SU-8, can change conformation during annealing, leading to increased helical organization and correspondingly increased CD values. Interestingly, they achieve much higher CD values than the pure PFBT film, even though the vast majority of the SU-8 encasing them has been removed. This suggests that the helical fibrils that have been liberated from the SU-8 matrix have much greater freedom to change supramolecular conformation than the fibrils in a pure PFBT film.

### 2.2. Dependence of Chiroptical Properties on Film Thickness

To further investigate the dramatic CD enhancement described above, we systematically compared the effect of annealing on the UV-vis and CD spectra of pure PFBT and PFBT/SU-8 films, as shown in **Figure 3**. The UV-Vis absorption spectrum of the PFBT/SU-8 film (Figure 3c) is similar to that of the pure PFBT film (Figure 3a), but the absorbance peak is slightly red-shifted, and increased UV absorbance is observed due to SU-8. The PFBT/SU-8 film consistently showed much larger CD (Figure 3d) than the pure PFBT film (Figure 3b).The shape of the CD spectrum is also different, with a bisignate feature in the pure PFBT and a monosignate feature in the nanocomposite, as discussed further below. The maximum CD increased further upon annealing at temperatures up to 150 °C, then decreased at

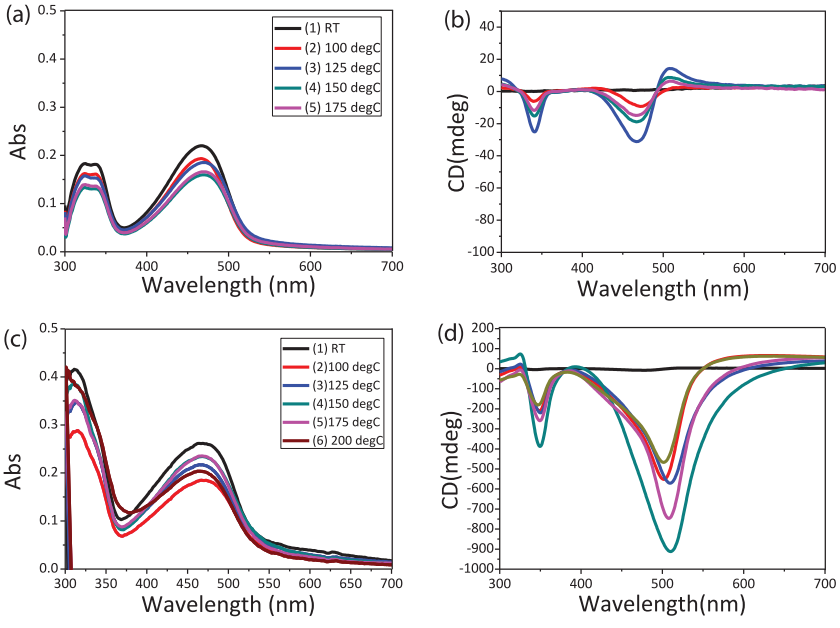


**Figure 3.** a,c) UV-vis absorption and b,d) CD spectra of a,b) PFBT films and c,d) PFBT/SU-8, 1/40 mass ratio, 20% solid content films (unpatterned and unexposed to UV) annealed at 100–175 °C for 15 min. Notice the dramatic difference in scale between (b) and (d).


© 2012 WILEY-VCH Verlag GmbH & Co. KGaA, Weinheim

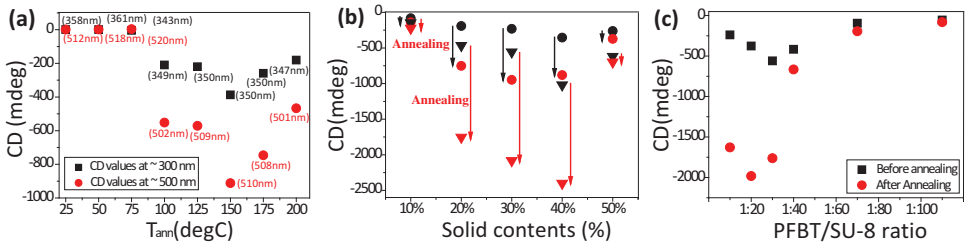


**Figure 4.** Maximum CD observed for two different CD bands of a) PFBT/SU-8 films 1/40 ratio, 20% solid content, dependence of the $CD_{max}$ values on annealing temperature (black symbols are $CD_{max}$ at short $\lambda_{max}$ and red symbols are $CD_{max}$ at longer $\lambda_{max}$), b) PFBT/SU-8 patterned film, 1/30 ratio, dependence of the $CD_{max}$ value on the thickness of the film remaining in the nominally unexposed areas (black symbols represent $CD_{max}$ before annealing and red colors after annealing, circles at $\lambda_{max} \approx 345$ nm, triangles at $\lambda_{max} \approx 490$ nm), and c) PFBT/SU-8 pattern ratio and annealing dependence of the $CD_{max}$ values at $\lambda_{max} \approx 490$ nm in 30% solid contents

higher temperature (Figure 3c,d). The effect of annealing on the maximum value of each CD peak is summarized in **Figure 4**a. Figure 4b and **Figure 5** show the dependence of the absorbance and CD spectra on film thickness, which was varied by changing the solid content from which the films were spin-coated. Here, film thicknesses of 0.25(1.0), 1.3(4.5), 1.7(7.0), and 2.2(9.0) µm, produced by spin-coating from solutions containing 10%, 20%, 30%, and 40% PFBT/SU-8 and photopatterning, were directly measured by SEM, as illustrated in **Figure 6**. The thicknesses listed are for the residual film left behind in the nominally unexposed regions; the thicknesses in the exposed regions are given in parenthesis. As the amount of PFBT/SU-8 was increased, the CD intensity increased more strongly than the absorbance. Both CD peaks, corresponding to $\pi$ to $\pi^*$ electronic transitions of PFBT at $\lambda_{max} \approx 345$ nm and $\lambda_{max} \approx 490$ nm, increased in similar proportion (Figure 4a,b). For solid content above 40%, the PFBT and SU-8 did not remain well dissolved and did not form a uniform film. Similar to pure chiral PFBT, the increase in CD intensity with film thickness was superlinear. This suggests that similar structural features are responsible for the observed CD effects in the nanocomposites as in pure chiral PFBT.[15]

We also varied the PFBT/SU-8 mass ratio to identify the value which yielded the highest CD. A clear change in the spectrum was apparent when PFBT/SU-8 composites with different ratios of chiral PFBT to SU-8 were compared (Figure 4c). Before annealing, the maximum CD value increased to $CD_{max}$ value of 600 mdeg as the PFBT/SU-8 ratio changed from 1/110 to 1/30 and then decreased as the PFBT/SU-8 ratio changed from 1/30 to 1/10 (Figure 4c). The maximum CD value of 2000 mdeg at 1/20 PFBT/SU-8 ratio is 77 times the CD value of pure PFBT after annealing. For nanocomposites at 1/110 to 1/40 mass ratios, annealing did not dramatically increase the CD values. However, annealing nanocomposites at 1/30 and 1/20 mass ratios produced very high CD signals of 1750 mdeg and 2000 mdeg, respectively. Thus, the chiroptical properties in the solid state developed after annealing the nanocomposite film in its thermotrophic phase. Nanocomposites with a 1/10 PFBT/SU-8 mass ratio did not show any further increase of the CD value. As such, the 1/20 PFBT/SU-8 mass ratio was found to be optimal for obtaining maximum CD. To determine whether the observed enhanced CD response of nanocomposites is due to true mesoscopic chirality, developed after annealing through formation of chiral aggregates (see detailed discussion below), or is partially due to propagation effects (pseudo chiral dichroism),[22] we converted the ellipticity spectra obtained for different film thicknesses to the spectral dependencies of the absorption dissymmetry ratio, $g_{abs}$, defined as $2(A_L - A_R)/(A_L + A_R)$, where $A_L$ and $A_R$ are the absorbances of left- and right circularly polarized light, respectively. In the case of true chirality, the dissymmetry ratio does not depend on film thickness.

The spectra of the dissymmetry ratio of nanocomposite films with four different thicknesses are shown in

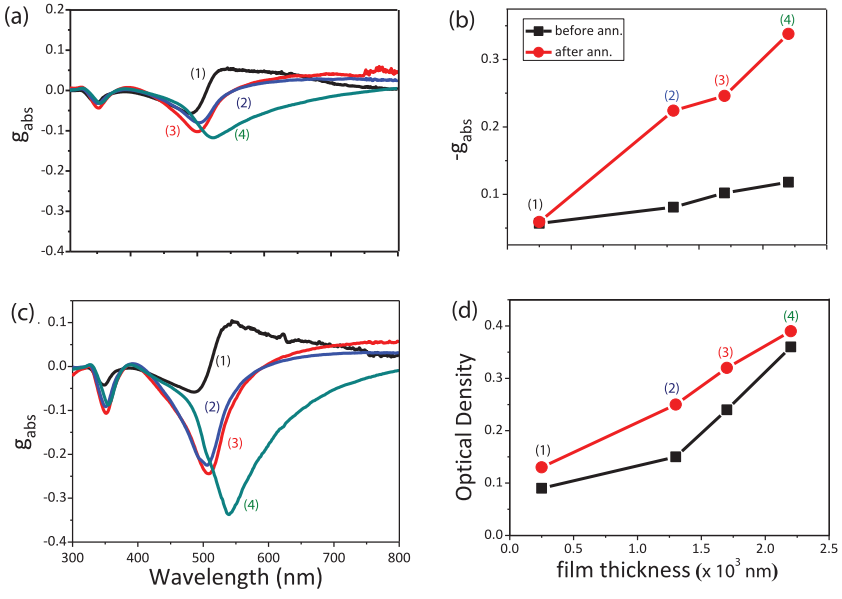


**Figure 5.** Dissymetry ratio spectra of photopatterned PFBT/SU-8 films, 1/30 ratio, nanocomposite for four different film thicknesses of 0.25, 1.3, 1.7, 2.2 µm: a) before annealing and c) after annealing, $T_{ann} = 150$ °C for 15 min. b) Absorption dissymmetry ratio, $g_{abs}$, versus film thickness, computed at the negative maximum of the spectra shown in panel (a). d) Optical density at $\lambda_{max}$ of absorption versus film thickness.


© 2012 WILEY-VCH Verlag GmbH & Co. KGaA, Weinheim

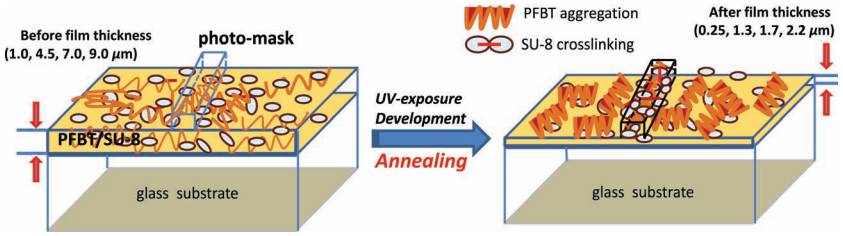


**Figure 6.** Schematic representation of thickness of patterned PFBT/SU-8 nanocomposite films. After UV exposure, development, and annealing, the residual film in the nominally unexposed regions was approximately ¼ of the thickness of the film prior to patterning.

Figure 5a,c, whereas the $g_{abs}$ values computed at the maxima of the negative lobes of CD spectra are shown in Figure 5b,d. The dependence of the g-factor on film thickness is rather weak for both annealed and non-annealed samples. At the same time, these dependencies do not saturate. For the thicknesses ranging from 250 nm to 2200 nm, $g_{abs}$ changes by about a factor of 6 in the case of the annealed film. This is less than proportional to the increase in film thickness, and is much smaller than that observed by Craig et al.[22] for the range of thicknesses from 40 nm to 300 nm, where there is no saturation. The value of $g_{abs}$ of an infinitely thin film can therefore be estimated by extrapolation of Section (2–3) (Figure 6b) to zero thickness. This value is about 0.05 for non-annealed film and 0.15 for the annealed one. The observed increase of g-factor with the thickness could be attributed to either propagation effects (pseudo chirality) or lesser degree of distortion of helical fibrils in thicker films. We did not use the 0.25 μm film in the extrapolation, noting that in this case the annealed and non-annealed films have the same value of $g_{abs}$, which indicates that the effect of annealing is inhibited in thin films. In this case, the film thickness is comparable to, or even smaller than, the size of the helical fibrillar structures observed in SEM (Figure 1). Therefore, the ordering of these fibrils in the 0.25 μm film cannot be expected to be the same as in the other films.

### 2.3. Mechanisms of Chirality Enhancement

The conjugated donor-acceptor alternating copolymer structure (fluorene-*alt*-benzothiadizole) of PFBT leads to two discrete absorption bands. The short-wavelength band centered at ≈325 nm is attributed to the π–π* and n-π* transitions of the conjugated aromatic segments, while the long wavelength absorption band centered at ≈473 nm can be assigned to intramolecular charge transfer (ICT) π–π* transitions of the backbone.[23] The well-known $S_0$-$S_1$ transition of poly(fluorene-*alt*-benzothiadizole) near 470 nm has been shown to occur due to an electron transfer from the fluorene unit to the benzothiadizole unit while the hole is somewhat delocalized on the π-conjugated backbone.[24] For both pure PFBT films and PFBT/SU-8 films, the absorbance band is broadened and red-shifted relative to that of the polymer in solution. This is attributed to the increased extent of π–π stacking alignment of the backbones, increased polarizability (because of planarization) of the film, or both.[25] Changes in UV-vis and CD spectra reflect the nature of these aggregates.[26–28] The main absorption bands of PFBT/SU-8 are shifted noticeably to the red as compared to films of pure PFBT; after annealing, the $\lambda_{max}$ were red shifted by ≈35 nm for SU-8/PFBT with respect to the pure PFBT.

The observed CD enhancement in SU-8/PFBT nanocomposites can be attributed to three possible mechanisms, as outlined below. The overall process of formation of a network of chiral polymer within the SU-8 photopolymer matrix and helical self-assembly during annealing is illustrated schematically in **Figure 7**. In order to rule out effects of linear dichroism (LD), we took LD spectra of representative samples. The LD signal was weak relative to the CD signal, as discussed further in supporting information, and we do not believe that LD is having any important effect on the results presented here.

The first mechanism of chirality enhancement can be associated with formation of chiral aggregates as in the case of the cyclopentanone/tetrahydrofuran spincoated films.[27–32] The transition from random coils to aggregates is a two-step process that proceeds via unaggregated, coplanar strands of PFBT. Upon decreasing the solvent quality, the absorption bands of SU-8/PFBT nanocomposites display a slight red shift and significant broadening. The red shift can be attributed to helical coiling of the π-conjugated backbone, originating from aggregation and stacking during solvent evaporation. Such a shift and broadening of the absorption band is commonly observed in ground-state charge-transfer complex (CTC) formation.[25] The CTC formation could result in an increase of the effective conjugation length (CL) of the polymer and hence the corresponding red shift of its absorption edge.[27]

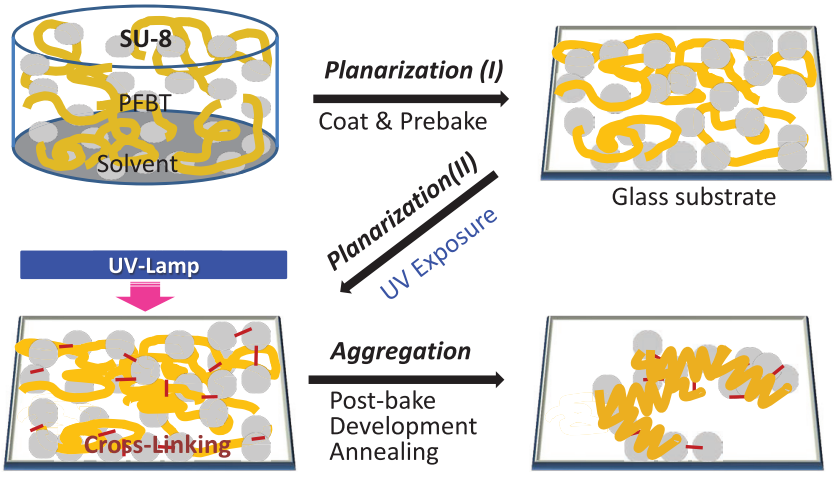


**Figure 7.** Overview of PFBT aggregation process resulting in helically-ordered PFBT/SU-8 nanocomposites with extraordinary optical activity.


© 2012 WILEY-VCH Verlag GmbH & Co. KGaA, Weinheim

The CD spectra of pure PFBT films (Figure 3b) in the visible range show a bisignate positive Cotton band (couplet) superimposed upon a negative Cotton band. The negative lobe of the effective couplet is centered at 471 nm in correspondence with the absorption maximum. Such a superposition implies conformational helicity of individual polymeric strands (producing a monosignate CD spectrum) and excitonic coupling in chiral aggregates (producing the bisignate feature).[33]

In contrast with pure PFBT films, PFBT/SU-8 nanocomposites demonstrate almost pure monosignate red-shifted negative Cotton bands. This is attributed to a dramatic enhancement of the red-shifted negative Cotton band superimposed upon the much weaker bisignate Cotton band. At the same time, the absorption spectra reveal slight bathochromic shifts and the appearance of a raised shoulder. This can be explained by formation of J-aggregates of helical polymeric strands (second mechanism of CD enhancement) within the SU-8 matrix. Thus, this suggests that the dominant mechanism of enhancement is supramolecular ordering to produce increased helicity in the nanocomposites, relative to the pure PFBT films.

Annealing of the patterned films (at 150 °C for 15 min) which contain large regions of PFBT/SU-8 aggregates that are free of the SU-8 matrix, resulted in a UV-vis spectrum in which the same bands are present, but with a small difference in the ratio of the intensities of the respective transitions. The CD spectrum, however, changed drastically. We attribute this to enhanced helicity of individual polymeric strands of PFBT as well as changes in the overall conformation of the fibrils, which have been liberated from the SU-8 matrix, but which remain as dispersed aggregates on the substrate, rather than a continuous smooth film (third mechanism of CD enhancement).

A sharp, red-shifted absorption band with corresponding monosignate Cotton effect has also been observed in other conjugated polymers. Swager and co-workers attributed this band to excitonic coupling in aggregates,[34] while Babudri et al. proposed that it originates from elongated helical strands confined within isolated domains.[33] Our observations support the latter interpretation.

## 3. Conclusions

In conclusion, we report on thin film fabrication of nanocomposites of a chiral $\pi$-conjugated polymer, PFBT, in a photopolymer matrix (SU-8). This optically clear nanocomposite shows exceptionally large circular dichroism caused by enhanced helical conformation of PFBT within the fully cured glassy SU-8 matrix. Key conclusions are that: 1) chiral PFBT/SU-8 nanocomposites give dramatically higher CD (up to $g_{abs}$ = -0.32) than pure PFBT films of the same optical density ($g_{abs}$ = -0.003); 2) chiral PFBT/SU-8 nanocomposites can be photopatterned, but the PFBT component is not fully removed under standard SU-8 processing conditions; and 3) chiral PFBT aggregates left behind after standard SU-8 development can exhibit dramatically higher CD than a smooth film containing the same amount of PFBT.

## 4. Experimental Section

PFBT was synthesized as a yellowish solid using palladium-catalyzed Suzuki polycondensation as the final step, and the crude product was purified with Soxhlet extractions with acetone over an 8 h period to obtain high molecular weight ($M_n$ = 13 000, $M_w$ = 30 000) PFBT. Its structure was confirmed by $^1$H NMR, GPC, and DSC, according to previously reported procedures.[15] PFBT was dissolved in THF for mixing with commercially available SU-8 2025 from MicroChem.

A PFBT solution in THF was added to 20% SU-8 2025 solution in cyclopentanone (CPO) and thoroughly mixed by mechanical stirring at 60 °C for 2 days. One hour before film fabrication, the solution was cooled to room temperature and sonicated for 3–5 min to remove dissolved air. Under dark condition, solutions of PFBT/SU-8 2025 in co-solvent (CPO/THF, 1/3) were spin coated on a glass substrate at 1000 rpm spin speed to form 1–9 μm thick films of SU-8 resist containing PFBT. Films were prebaked at 95 °C for 5 min. A Karl Suss UV aligner with 365 nm exposure wavelength was used for lithography, through a mask with a checkerboard pattern of about 12.5% exposed area. The samples were post-baked at 95 °C for 5 min and then developed with PGMEA (propylene glycol methyl ether acetate) and rinsed with 2-propanol. The UV-vis absorbance and CD spectra were measured in transmission using a Shimadzu 3101 UV-vis spectrophotometer and a Jasco J-815 CD spectrometer, respectively, before and after annealing of the films at various temperature (≈100 to 200 °C) for 15 min under argon atmosphere.

## Supporting Information

Supporting Information is available from the Wiley Online Library or from the author.

## Acknowledgements

This work was supported in part by a grant from the Air Force Office of Scientific Research (grant no. FA95500610398). The authors thank Prof. John Cerne for assistance with linear dichroism measurements.

Received: May 10, 2012
Revised: June 23, 2012
Published online: July 27, 2012

[1] T. A. Skotheim, J. R. Reynolds, *Handbook of conducting polymers. Conjugated polymers: theory, synthesis, properties, and characterization*, 3rd ed., CRC Press, Boca Raton **2007**.
[2] B. Pal, W. C. Yen, J. S. Yang, W. F. Su, *Macromolecules* **2007**, *40*, 8189.
[3] S. Inagi, S. Hayashi, K. Hosaka, T. Fuchigami, *Macromolecules* **2009**, *42*, 3881.
[4] M. H. Chen, J. Hou, Z. Hong, G. Yang, S. Sista, L. M. Chen, Y. Yang, *Adv. Mater.* **2009**, *21*, 4238.
[5] Y. J. Cheng, S. H. Yang, C. S. Hsu, *Chem. Rev.* **2009**, *109*, 5868.
[6] A. C. Grimsdale, K. L. Chan, R. E. Martin, P. G. Jokisz, A. B. Holmes, *Chem. Rev.* **2009**, *109*, 897.
[7] J. J. Wei, C. Schafmeister, G. Bird, A. Paul, R. Naaman, D. H. Waldeck, *J. Phys. Chem. B* **2006**, *110*, 1301.
[8] V. Percec, M. Glodde, T. K. Bera, Y. Miura, I. Shiyanovskaya, K. D. Singer, V. S. K. Balagurusamy, P. A. Heiney, I. Schnell, A. Rapp, H. W. Spiess, S. D. Hudson, H. Duan, *Nature* **2002**, *419*, 384.
[9] H. Engelkamp, S. Middelbeek, R. J. M. Nolte, *Science* **1999**, *284*, 785.
[10] S. d. Zouhdi, A. Sihvola, A. P. Vinogradov, *Metamaterials and plasmonics: fundamentals, modelling, applications: [proceedings of the NATO Advanced Research Workshop on Metamaterials for Secure Information and Communication Technologies*, Marrakech, Morocco, 7–10 May 2008], Springer, Dordrecht, Netherlands **2009**.


© 2012 WILEY-VCH Verlag GmbH & Co. KGaA, Weinheim

[11] B. N. Wang, J. F. Zhou, T. Koschny, M. Kafesaki, C. M. Soukoulis, *J. Opt. A: Pure Appl. Opt.* **2009**, *11*, 114003.
[12] S. Tretyakov, A. Sihvola, L. Jylhä, *Photonics Nanostruct. Fundam. Appl.* **2005**, *3*, 107.
[13] Y. M. Liu, X. Zhang, *Chem. Soc. Rev.* **2011**, *40*, 2494.
[14] R. Abbel, A. Schenning, E. W. Meijer, *Macromolecules* **2008**, *41*, 7497.
[15] H. S. Oh, S. Liu, H. Jee, A. Baev, M. T. Swihart, P. N. Prasad, *J. Am. Chem. Soc.* **2010**, *132*, 17346.
[16] K. Okamoto, P. Chithra, G. J. Richards, J. P. Hill, K. Ariga, *Int. J. Mol. Sci.* **2009**, *10*, 1950.
[17] K. Terao, Y. Mori, T. Dobashi, T. Sato, A. Teramoto, M. Fujiki, *Langmuir* **2004**, *20*, 306.
[18] T. Fukushima, K. Tsuchihara, *Macromol. Rapid Commun.* **2009**, *30*, 1334.
[19] W. H. Teh, U. Durig, U. Drechsler, C. G. Smith, H. J. Guntherodt, *J. Appl. Phys.* **2005**, *97*, 64104.
[20] J. Kim, M. G. Allen, Y. K. Yoon, *J. Micromech. Microeng.* **2011**, *21*, 035003.
[21] A. F. Lasagni, D. J. Yuan, S. Das, *Adv. Eng. Mater.* **2009**, *11*, 408.
[22] M. R. Craig, P. Jonkheijm, S. C. J. Meskers, A. Schenning, E. W. Meijer, *Adv. Mater.* **2003**, *15*, 1435.
[23] G. Qian, H. Abu, Z. Y. Wang, *J. Mater. Chem.* **2011**, *21*, 7678.
[24] K. G. Jespersen, W. J. D. Beenken, Y. Zaushitsyn, A. Yartsev, M. Andersson, T. Pullerits, V. Sundstrom, *J. Chem. Phys.* **2004**, *121*, 12613.
[25] Z. G. Zhang, K. L. Zhang, G. Liu, C. X. Zhu, K. G. Neoh, E. T. Kang, *Macromolecules* **2009**, *42*, 3104.
[26] C. R. G. Grenier, S. J. George, T. J. Joncheray, E. W. Meijer, J. R. Reynolds, *J. Am. Chem. Soc.* **2007**, *129*, 10694.
[27] E. Yashima, K. Maeda, H. Iida, Y. Furusho, K. Nagai, *Chem. Rev.* **2009**, *109*, 6102.
[28] N. Berova, K. J. Nakanishi, R. Woody, *Circular dichroism: principles and applications*, 2nd ed., Wiley-VCH, New York **2000**.
[29] C. Gautier, T. Burgi, *J. Am. Chem. Soc.* **2008**, *130*, 7077.
[30] B. M. W. Langeveld-Voss, R. A. J. Janssen, E. W. Meijer, *J. Mol. Struct.* **2000**, *521*, 285.
[31] M. O. Osotov, V. V. Bruevich, D. Y. Paraschuk, *J. Chem. Phys.* **2009**, *131*, 094906.
[32] S. Vandeleene, K. Van den Bergh, T. Verbiest, G. Koeckelberghs, *Macromolecules* **2008**, *41*, 5123.
[33] F. Babudri, D. Colangiuli, L. Di Bari, G. M. Farinola, O. H. Omar, F. Naso, G. Pescitelli, *Macromolecules* **2006**, *39*, 5206.
[34] S. Zahn, T. M. Swager, *Angew. Chem. Int. Ed.* **2002**, *41*, 4225.
[35] A. Baev, M. Samoc, P. N. Prasad, M. Krykunov, J. Autschbach, *Opt. Express* **2007**, *15*, 5730.
[36] M. Krykunov, M. D. Kundrat, J. Autschbach, *J. Chem. Phys.* **2006**, *125*, 194110.


© 2012 WILEY-VCH Verlag GmbH & Co. KGaA, Weinheim